



Universiteit Utrecht

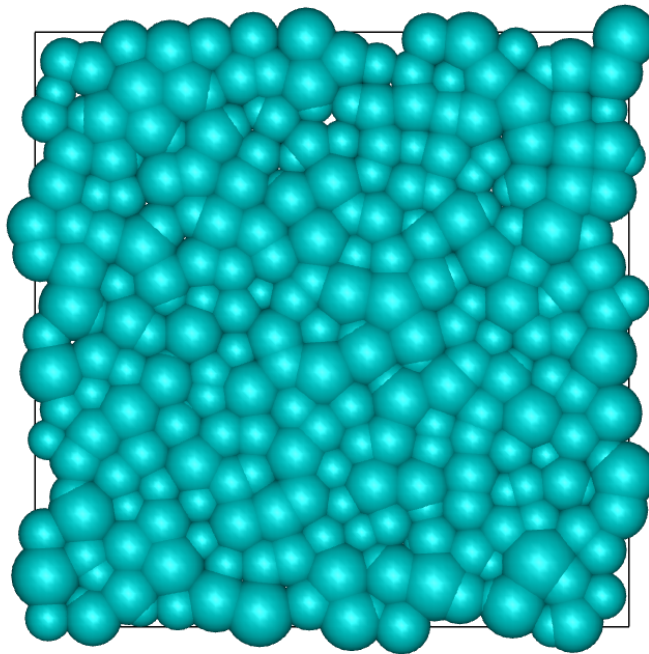
Faculteit Bètawetenschappen

Modelling the Dynamics of Epithelial Tissue

BACHELOR THESIS

Thijs ter Rele

Natuur- en Sterrenkunde



Supervisor:

Dr. Joost de Graaf
Instituut voor Theoretische Fysica

Daily supervisor:

MSc. Meike Bos
Instituut voor Theoretische Fysica

June 12, 2020

Abstract

Jamming behaviour has been observed in epithelial tissue. We tried to get more insight into jamming behaviour in monolayers of cells through numerical modelling. In our simulation epithelial cells were modelled as soft-potential spheres and soft-potential dumbbells. Oscillations in cell length and size were used to study the effect of deformation of cells on the collective dynamics of epithelial tissue. Jamming was observed in systems of passive disks, but jamming disappeared as cell oscillations were introduced. All simulated systems with dumbbells were linearly diffusive. Adding oscillations to the dumbbells increased the diffusivity of the system, especially at higher densities. The model of oscillating dumbbells used in this thesis was successful in showing the effect of oscillations on the dynamics of diffusive systems. However, it did not succeed in simulating jamming. For future research it will be necessary to look further into creating a different model of deforming epithelial cells if we want to study jamming behaviour.

Contents

1	Introduction	1
2	Background	2
2.1	Epithelial Cells	2
2.2	Jamming and Glass Transitions	2
3	Method	4
3.1	Overview of the simulation	4
3.2	Brownian Motion	4
3.3	Interactions	5
3.4	Cell Lists	5
3.5	Dumbbell Particles	6
3.6	Analysis	6
3.6.1	Mean Squared Displacement	6
3.6.2	Self-intermediate Scattering Function	8
3.7	Simulation Parameters	8
3.8	Checking Simulation Accuracy	9
4	Results	12
4.1	Passive Particles	12
4.2	Oscillating Particles	17
4.2.1	Oscillating Dumbbells	18
5	Discussion	20
6	Conclusion	22
	References	I

1 Introduction

Cell dynamics play a part in biological processes. Wound healing, embryonic development and progression of cancer are influenced by the collective dynamics of cell systems[1]. These three processes rely on the motion of cell tissue in a fluid-like manner, but also on subsequent solidification of cell tissue. The behaviour of cell tissue in two-dimensional monolayers, such as epithelial tissue, in these processes suggest that transitions between a fluid-like phase and a jammed phase take place[2]. Epithelial cells have been observed to undergo these phase transitions between jammed and unjammed states[3]. In a jammed state the constituents that make up a system are caged by other constituents and cannot move. We are interested in these collective dynamics in a layer of epithelial cells.

In the section Background we will provide some information on epithelial cells and jamming. Epithelial cells can deform through accumulation and generation of forces on the cytoskeletons in the cells. These cell deformations can be periodic, leading to cell shape oscillations[4]. It has been observed that the expansions and contractions of neighbouring cells are correlated[5]. Interactions between neighbouring cells also play a role in the deformation of individual cells[6]. We want to study the influence of cell oscillations on the collective dynamics of cell tissue. We are interested if these deformations have any effect on the jamming of the system. Therefore, we will try to answer the following question in this bachelor thesis: *what is the effect of cell oscillations on the collective dynamics of a two-dimensional epithelial tissue?*

In the Method section we will explain how the simulation is set up. We built a simulation of soft-potential particles to answer this question. We used a two-dimensional simulation with periodic boundary conditions. The motion of the particles is simulated using damped Brownian dynamics, which means that random thermal fluctuations are included in the motion of the particles. Dumbbell-shaped particles were used in this simulation, which were constructed by connecting pairs of disk-shaped colloids with a spring force. We introduced oscillations in length of the dumbbells and oscillations in size of the individual particles to simulate deformations. The dumbbells were used to model deformations of a cell. These deformations were modelled by tuning the oscillations of two connected disks.

In the Results section we show the findings from the simulations. We did not observe jamming in any of the simulated systems of dumbbells. We did however find that dumbbell oscillations had an effect on the dynamics of the systems. Both dumbbell-length oscillations and particle size-oscillations increased the diffusivity of the system at intermediate and high densities of $\rho > 1.4$. At intermediate densities of around $\rho = 1.8$ the effect of length oscillations to the diffusivity was much larger than the effect of particle size oscillations. At very high densities of $\rho = 3.0$ the diffusivity increase by particle size oscillations increased, although the effect was still smaller than the effect of length oscillations. From these simulation we conclude that cell oscillations increase the diffusivity of systems of epithelial cells at high densities. The effect of length oscillations is larger than the effect of disk size oscillations, although size oscillations play a larger role at higher densities.

In the Discussion section the results are discussed further. Using the simulations we were able to study the effect of cell oscillations on fluid-like systems. However, we did not encounter jammed systems, even when we used passive particles. A possible cause for the absence of jamming is that the potential used in creating disks was not stiff enough. It would be interesting to determine the effect of a different type of dumbbell potential on jamming of the system. Another possibility for future research is to compare the results of Brownian dynamics simulations with the results of non-thermal dynamics simulations.

2 Background

In this section the background of the research question will be briefly sketched. First we give some information on the behaviour of epithelial cells. Next we explain what jammed systems and glassy systems are and why jamming behaviour is relevant in cell tissue.

2.1 Epithelial Cells

Epithelial cells, or epithelial tissue, are one of the four types of human tissue. Epithelial cells cover body surfaces, line body cavities and form solid glands. Examples of epithelial tissue are skin tissue and blood vessel lining[7]. Epithelial tissue often consists of a single layer of epithelial cells on top of another type of tissue, as can be seen in figure 1. The cells making up the tissue are linked together by cell junctions into a functional unit. There are three types of junctions: anchoring, occluding and communicating junctions. Anchoring junctions give the epithelial tissue mechanical strength, by linking the cytoskeletons of the cells together. Occluding junctions bind the cells together to maintain the integrity of the cell tissue. The occluding junction also serves to prevent diffusion of individual cells. The third junction type, the communicating junction, allows movement of molecules between cells[7].

The shape and size of epithelial cells can fluctuate. Changes in shape and size of the cells are governed by the acto-myosin cytoskeleton[8]. Acto-myosin is a protein-complex which produces contractile forces in a cell[7]. The cytoskeleton can best be seen as a network of spokes that can contract and expand, changing the shape and size of the cell. In cells of tissues undergoing morphogenesis cytoskeletons show periodic contractions leading to cell shape oscillations. Experimental work has shown that these cell deformations are largely autonomous[4]. At the same time forces are exerted on a cell by neighbouring cells through anchoring junctions[7]. Through these cell connections deformations are transmitted between cells[6]. In this thesis therefore we will study systems of oscillating cells, combined with forces from neighbouring cells.

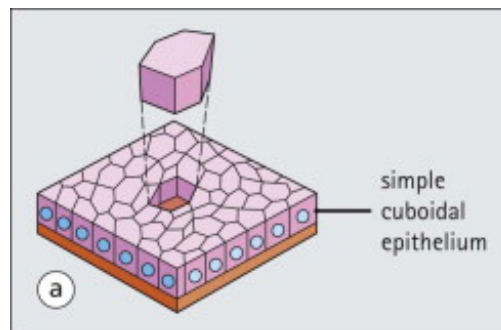


Figure 1: Diagram of epithelial tissue. The pink blocks represent epithelial cells, each with a blue nucleus, and the orange slab represents the underlying tissue. The structure of epithelial cells completely covers the underlying surface. Reprinted from [7] with permission from Elsevier.

2.2 Jamming and Glass Transitions

Jamming transitions and glass transitions are types of phase transitions from a fluid-like phase to a solid-like phase[9]. These transitions are both defined by the sudden stop of the dynamics of the system. In glasses and jammed systems alike the constituents of the system are trapped in a cage of neighbouring particles that prevents the constituents from moving. The disordered structure of the fluid however stays intact in glasses and jammed systems[10]. This is different from normal crystallisation, where the dynamics also stop but the particles are positioned on an ordered lattice. Examples of these systems can be found in traffic, foam and grains of sand[11].

Glass transitions and jamming transitions do however differ from each other. A major difference is that thermal fluctuations to the motion of the system's constituents do not play a role in jamming, but they do in glass transitions. In jammed systems only mechanical forces play a role[12]. The similarity between jamming and glass transitions has led to some attempting to combine the two transitions into a single model[11].

Jamming behaviour occurs in cell tissue. It seems that jammed behaviour plays a role in processes in which collective cell migration takes place, such as wound healing, embryonic development and cancer progression[1]. In these processes cells first spread out in a fluid-like manner, but later solidify. Tissues undergoing these processes have a solid-like character over short time-steps and a collective flow character over longer time steps. This indicates that jamming plays role in these processes[2]. When dealing with jamming in living tissue one has to take two factors in consideration. The first factor is that living tissue normally has a fixed volume with a volume fraction of 1.0, or in the case of two-dimensional tissues it has a fixed area. This means that the cells exactly cover the entire skin area. The second factor is that living tissue has a fixed temperature. Hence changes in temperature or in volume fraction are probably not the cause of jamming transitions in tissues. It is more likely that the causes for a jamming transition are cell shape, interaction forces between cells, active movement of the cells themselves and applied stresses on the system[1].

Jamming has been simulated in systems consisting of soft-potential disks. In the simulations of soft-disks the jamming transition was sudden and well defined[13]. Jamming has also been simulated in two-dimensional systems of soft ellipsoids and in systems of soft rigid dumbbells[14].

Because of the similarity between glass and jamming transitions we refer to both transitions as jamming in this thesis. However, we do take temperature and thermal fluctuations into consideration because thermal fluctuations are present in the motion of cells on microscale. There are two reasons why we refer to both transitions as jamming transitions. The first reason is that mechanical forces are dominant in our simulations. In this thesis we simulate oscillating epithelial cells at high density. Epithelial cells are of a scale of $10 \mu m$, which means that motion due to thermal fluctuations is small. At high densities for these size particles thermal fluctuations are much smaller than mechanical forces. The second reason is that halting behaviour in cells is mostly referred to as jamming[1][15]. Hence, we have chosen to refer to halting of dynamics as jamming.

3 Method

To study the behaviour of cells with oscillating size, we made a simulation of interacting disks and a simulation of interacting dumbbells. We first give a general overview of the model used in this thesis. We then go on to discuss in greater detail how to simulate Brownian motion and interactions between particles using cell lists. After this we describe how the dumbbells in the simulation were built. We also describe how we analysed the simulations. In the final section we check if the simulation had been implemented properly.

3.1 Overview of the simulation

The simulation used in this bachelor thesis is a simulation of polydisperse particles in two dimensions. We apply periodic boundary conditions on the particles. This simulation is meant to be a general simulation of the motion of epithelial cells. The simulation therefore includes many factors that have a possible influence on the motion of the cells. These include thermal fluctuations, cell shape oscillations, cell size oscillations and interactions between cells.

The motion of the particles is simulated using damped Brownian dynamics and the particles interact with each other with a Hertz potential. Two types of particles are used in separate simulations. The first type is a soft-potential disk, which represents regular cells. The second type is a soft-potential dumbbell, which represents deforming cells. The dumbbells consist of two disks connected by a spring with an adjustable equilibrium length. We study two types of oscillations. The first type of oscillation is the oscillation of the diameter of the individual disks that make up a dumbbell. The second type of oscillation is the oscillation of the distance between the two disks of a dumbbell.

3.2 Brownian Motion

We model the motion of cells with a simulation of disks. The cells are of the order size of $10 \mu m$ and are suspended in a fluid. Because the cells undergo collisions with the fluid molecules, they experience Brownian motion. Instead of simulating all individual water molecules we use Brownian dynamics to simulate the motion of the disks. The collisions with the fluid molecules are modelled as an effective random force on the disks. This random force is normally distributed and given using the Gaussian term $\mathbf{R}(t)$. The factor $\mathbf{R}(t)$ has a mean $\langle R_i(t) \rangle = 0$ and squared mean $\langle R_i(t)R_j(t') \rangle = \delta(t-t')\delta_{ij}$, for $i, j \in \{x, y, z\}$.

Colloids have a low Reynolds number, which means that the frictional forces on a particle are much larger than the inertial forces. This leads to damped Brownian motion, for which the inertial term disappears from the equation of motion. Damped motion is described by the Langevin equation:

$$\dot{\mathbf{x}} = \sqrt{\frac{2k_B T}{\gamma}} \mathbf{R}(t) + \frac{1}{\gamma} \mathbf{F}_{\text{int}}. \quad (3.1)$$

In equation 3.1 \mathbf{F}_{int} is the force exerted on a particle caused by interactions with other particles. The first term on the right hand side adds the random behaviour of particle motion in Brownian dynamics. γ is the friction coefficient, which determines the friction the disks experience while moving in the fluid. For spherical particles $\gamma = 6\pi\eta a$, with a the radius of the particles and η the viscosity of the fluid in which the particles are suspended.

To apply equation 3.1 to a simulation, we use the Euler-Mayurama method. This method is used, because a stochastic variable is present in the equation. To determine the new position of a disk in the simulation, we use the formula

$$\mathbf{x}(t + \Delta t) = \mathbf{x}(t) + \sqrt{2D_0} \mathbf{\Gamma}(t) \sqrt{\Delta t} + \frac{1}{\gamma} \mathbf{F}_{\text{int}} \Delta t, \quad (3.2)$$

where $\mathbf{\Gamma}(t)$ is a Gaussian random number in two dimensions and $D_0 = \frac{k_B T}{\gamma}$ is the diffusion constant for Brownian motion. In the second term on the right hand side we multiply by $\sqrt{\Delta t}$ instead of Δt . We multiply by Δt because the Gaussian position distribution of particles should have a width of $\sqrt{2D_0 \Delta t}$ after time period Δt . The evolution of the system can be simulated with this equation of motion.

3.3 Interactions

In the simulation the disks interact with each other with the Hertz potential, which is a bounded soft potential. The Hertz potential describes the change in elastic energy of two deformable objects, when subjected to axial compression[16]. The potential has form

$$V(r) = \begin{cases} 0, & \text{if } r > \sigma \\ \epsilon \left(1 - \frac{r}{\sigma}\right)^{5/2}, & \text{if } r < \sigma, \end{cases} \quad (3.3)$$

with σ and ϵ respectively being the length and energy scale. Length scale σ is the average diameter of two interacting disks. Because the disks are polydisperse, this σ is different for every interaction. r represents the distance between the centres of two disks. For the Brownian dynamics simulation, we need to derive the force between particles as a result of this potential. The potential in equation 3.3 leads to the interaction force

$$\mathbf{F}(\mathbf{r}_{ij}) = \frac{5}{2} \frac{\epsilon}{\sigma r} \left(1 - \frac{r}{\sigma}\right)^{3/2} \mathbf{r}_{ij}, \quad (3.4)$$

with $\mathbf{r}_{ij} = \mathbf{r}_j - \mathbf{r}_i$ the vector between particles i and j and with r the length of this vector. This force is used as interaction force in equation 3.2.

3.4 Cell Lists

To determine the total force on a disk due to interactions, it is necessary to compare the position of a disk with the positions of all other disks. However, comparing the position of every disk to the position of every other disk is computationally intensive. Only the disks that are at a distance $r < \sigma$ from a certain disk contribute to the total force on that disk. Hence we implemented a cell list algorithm using linked lists. This algorithm divides up the simulation box into multiple smaller square cells, as can be seen in figure 2. Each disk is assigned to the cell in which it is located. The cell size is such that a disk can only interact with other disks in its own and its neighbouring cells. It is therefore required that the cell size L_c is larger than σ . We only need to compare the position of a certain disk with the positions of disks in neighbouring cells (the 8 grey cells in figure 2) and of other disks in the same cell (the yellow cell), instead of comparing with every disk. This is computationally less intensive, especially for simulations with larger numbers of disks. The cell lists are updated when a disk changes cell. Only the former and new cell of the moved disk are updated.

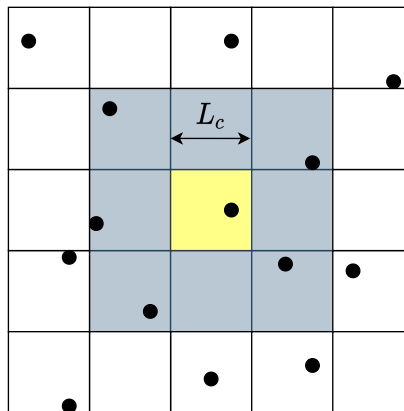


Figure 2: Schematic of the construction of cell lists, based upon a similar figure in [17]. The particle in the yellow cell can only interact with other particles its own cell (yellow cell) and neighbouring cells (grey cells). L_c indicates the length of a cell, which has to be larger than disk diameter σ .

3.5 Dumbbell Particles

To study phase shifts between neighbouring cells, we create dumbbell particles out of two disks of equal equilibrium size diameter, as can be seen in figure 3. We connect two disks with a spring force

$$F_{\text{spring}} = -k(r_{ij} - L(t)) \mathbf{r}_{ij}, \quad (3.5)$$

where k is the spring constant, $L(t)$ the equilibrium length of the spring and $r_{ij} = |\mathbf{r}_i - \mathbf{r}_j|$ the distance between the two disks. The diameter of a disk in a dumbbell is given by $\sigma(t)$. The disks in a dumbbell do not have to have the same diameter $\sigma(t)$. Two connected disks only interact with each other by this spring force. This spring force allows the disks to rotate around each other, which means that the dumbbell itself rotates. The dumbbells have a dimensionless aspect ratio $L^* = L/\sigma$. In simulating dumbbells a couple

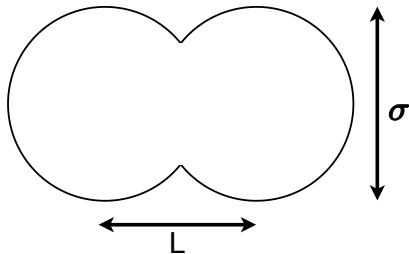


Figure 3: Shape of a dumbbell constructed from two disks. L is the distance between the two disks, σ is the disk diameter.

parameters can be tuned. The equilibrium length $L(t)$ can be set to oscillate, which means that the length of the dumbbell oscillates. The second parameter that can be tuned is the diameter $\sigma(t)$ of a disk in a dumbbell. In simulations both disks oscillate with the same frequency. The oscillations of the two disks in a dumbbell have a set phase difference of $\phi = \pi$, which is half of a total oscillation cycle. If one disk decreases in size, the other disk increases in size. The total length of the dumbbell is therefore conserved if $L(t)$ is kept constant. We performed four types of oscillations on dumbbells in this thesis. One simulation was performed using passive dumbbells. The second one was a simulation using dumbbells with length oscillations. All dumbbells oscillated with the same frequency, but each oscillated with a random phase difference. The third simulation used dumbbells with oscillating disk size. The disks all oscillated with the same frequency and again each dumbbell oscillated with a random phase difference. In the fourth simulation we combined the two types oscillations. The length oscillations and disk oscillations in a single dumbbell had the same phase difference.

3.6 Analysis

We wanted to determine under what parameters a system becomes jammed. It was necessary to be able to differentiate a jammed system from an unjammed one. We used mean squared displacement and the self-intermediate scattering function to investigate if a system was jammed or unjammed.

It is possible that the system as a whole moves, instead of individual particles. This will affect measurements. We therefore made comparisons between snapshots of the simulation using the disk-positions with respect to the centre of mass of the system. Using centre-of-mass coordinates cancels out any total movement of the system on the measurements.

3.6.1 Mean Squared Displacement

We determined the mean squared displacement (MSD) of the particles. The MSD is the average squared distance a particle has moved from its initial position in a period Δt . The MSD indicates how far particles move and is therefore a good indicator for determining if the particles are caged. It is calculated using

$$\langle \mathbf{r}^2 \rangle(\Delta t) = \frac{1}{N_j} \frac{1}{N} \sum_j \sum_i (\mathbf{r}_i(\Delta t + t_j) - \mathbf{r}_i(t_j)). \quad (3.6)$$

In equation 3.6 N_j is the number of comparisons between time steps we can make. N_j decreases as time step Δt increases. The minimum number used in determining the MSD is $N_j = 4720$. For dumbbells we use the centre of mass of a dumbbell as the reference point.

We performed five runs for each set of parameters to obtain better statistics. We then took the average of these five runs at every time step. We used the average value to determine the standard error of this average by taking

$$s = \frac{1}{N_{\text{runs}}} \left[\frac{1}{N_{\text{runs}} - 1} \sum_i^{N_{\text{runs}}} \left(\langle \mathbf{r}^2 \rangle_{\text{average}} - \langle \mathbf{r}^2 \rangle_i \right)^2 \right]. \quad (3.7)$$

If we set $\mathbf{F}_{\text{int}} = 0$, we can determine the mean displacement $\langle x \rangle$ and MSD $\langle x^2 \rangle$ exactly using integration. The calculations below are done for one dimension.

$$\begin{aligned} x &= \int_0^t dt' \dot{x}(t') = \sqrt{\frac{2k_B T}{\gamma}} \int_0^t dt' R(t') \\ \langle x \rangle &= \sqrt{\frac{2k_B T}{\gamma}} \int_0^t dt' \langle R(t') \rangle = 0 \\ x^2 &= x(t)x(t) = \int_0^t dt' \dot{x}(t') \dot{x}(t') = \frac{2k_B T}{\gamma} \int_0^t dt' R(t') R(t') \\ \langle x^2 \rangle &= \frac{2k_B T}{\gamma} \int_0^t dt' \langle R(t') R(t') \rangle = \frac{2k_B T}{\gamma} t. \end{aligned}$$

In the case that particles can move in more than one dimension, the MSD is

$$\langle \mathbf{x}^2 \rangle = \frac{2dk_B T}{\gamma} t = 2dD_0 t, \quad (3.8)$$

with d being the number of dimensions. $D_0 = \frac{k_B T}{\gamma}$ is the diffusion constant for Brownian motion without interactions between particles. When particles do interact, the diffusion constant differs from D_0 . D_0 is used as a reference point in analysis of diffusion.

Typical MSD-curves for a jammed and an unjammed system are shown in figure 4. An unjammed, fluid system will have linear diffusion and therefore a linear increase in MSD. The slope of the MSD is constant in this case. This is described in equation 3.8. The MSD of a jammed system will plateau after a certain time step. This plateauing occurs when the MSD becomes larger than the squared size of the confining cage in which a disk is jammed.

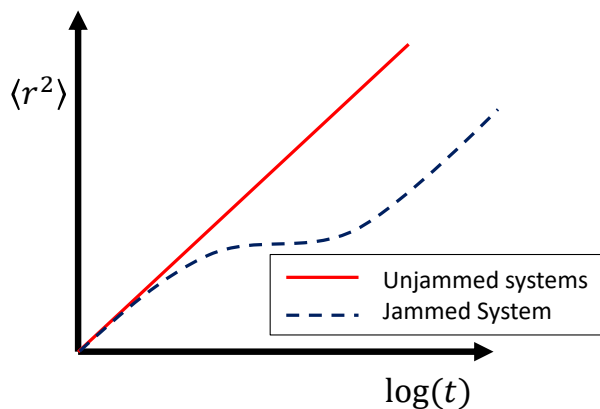


Figure 4: Typical curves of the mean squared displacement against time for an unjammed system and a jammed system, as indicated in the legend.

3.6.2 Self-intermediate Scattering Function

The second method we used to determine if a system is jammed or unjammed, is the self-intermediate scattering function. To produce the results for the self-intermediate scattering function results we first need to determine the structure factor $S(\mathbf{q})$ of a snapshot of the system. $S(\mathbf{q})$ is derived by Fourier transforming the radial distribution function $g(r)$. The radial distribution function shows the average density at a distance of a single particle by taking $g(r)\bar{\rho}$. The structure factor $S(\mathbf{q})$, which can be obtained experimentally through scattering experiments, can be determined through Fourier transform by taking

$$S(\mathbf{q}) = 1 + \bar{\rho} \int d\mathbf{r} \exp[i\mathbf{q} \cdot \mathbf{r}]g(r). \quad (3.9)$$

We take the \mathbf{q} -vector at which the structure-factor has its first peak. We then use this \mathbf{q} -vector to determine the self-intermediate scattering function as follows:

$$F_s(\mathbf{q}, t) = \frac{1}{N} \left\langle \sum_{j=1}^N \exp[i\mathbf{q} \cdot (\mathbf{r}_j(t) - \mathbf{r}_j(0))] \right\rangle. \quad (3.10)$$

Centre-of-mass coordinates were used in determining F_s . We only plotted the real part of this equation. The self-intermediate scattering function relates the position of particles at time $t' = t$ with its position at time $t' = 0$. It correlates these two positions with each other. Typical curves for a jammed system and for an unjammed system are plotted in figure 5. F_s is larger when the position of the particles at time t corresponds more with its initial position. In an unjammed system F_s quickly goes to zero. In a jammed system the system first decreases quickly, but afterwards plateaus for larger time steps. As F_s plateaus the two positions do not decorrelate any more.

In this thesis we used code provided by Clara Abaurrea-Velasco to produce the self-intermediate scattering function from systems of colloids.

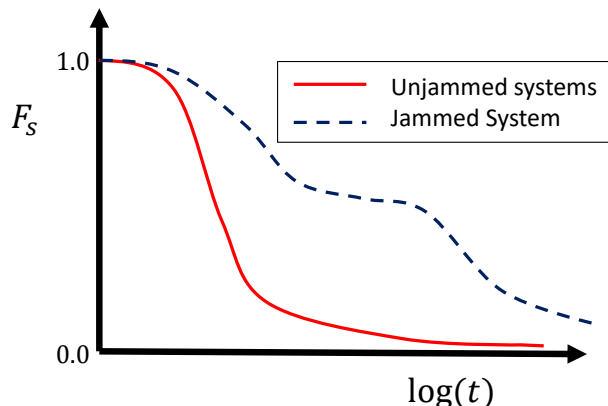


Figure 5: Typical curves of the self-intermediate structure factor against time for a non-jammed system and a jammed system, as indicated in the legend.

3.7 Simulation Parameters

A series of simulations have been performed on passive and active Hertzian disks. The simulations have been done with 256 disks for $5 * 10^6$ steps at multiple densities between $\rho = 1.0$ and $\rho = 3.0$. The time step was set to $\Delta t = 0.0001 = 10^{-4}t_{\text{dif}}$. Diffusion time is given by $t_{\text{dif}} = \frac{\sigma^2}{D_0}$.

The following parameters, which are also given in table 1, were used in the simulation. The disks had an average diameter of σ . The polydispersity of the disks was normally distributed with a standard deviation of $s = 0.1\sigma$. The equilibrium distance between 2 disks that make up a dumbbell was $L = 0.6\sigma$, which means that the aspect ratio was $L^* = 0.6$. These disks were connected by a spring of spring constant $k = 1000 1/t_{\text{dif}}^2$.

The ratio between the temperature and energy scale was set to $\frac{\epsilon}{k_B T} = 200$. The viscosity of the fluid was set to $\eta = \frac{1}{3\pi}$, so that the friction coefficient of the fluid becomes $\gamma = 6\pi\eta a = 1$. This means that standard diffusion coefficient used in equation 3.8 was $D_0 = 1.0$. We therefore simulated 500 diffusion times t_{dif} . We added oscillations of the disk diameter of $\Delta\sigma = 0$ and $\Delta\sigma = 0.2$ and oscillations of the dumbbell length of $\Delta L = 0$ and $\Delta L = 0.2$. These oscillations both had frequency $\nu = 10.0$ $1/t_{\text{dif}}$.

Parameter	$\frac{\epsilon}{k_B T}$	η	s	L	k	Δt	ν
Value	200	$\frac{1}{3\pi}$	0.1σ	0.6	1000.0	10^{-4}	10.0

Table 1: The parameters used in the simulations.

3.8 Checking Simulation Accuracy

To determine if the simulation was functioning properly we performed some tests. We needed to determine if the Brownian dynamics and the interactions between particles using cell lists had been implemented properly. These test were done using ordinary disks.

A good test for the Brownian dynamics in the simulation is to set interaction forces to zero and check if the diffusion coefficient is as expected. In figure 6 the MSD of 256 particles is plotted. The expectation was that the MSD was described by $\langle r^2 \rangle = 4t$ under the given conditions. The results in figure 6 match with this prediction.

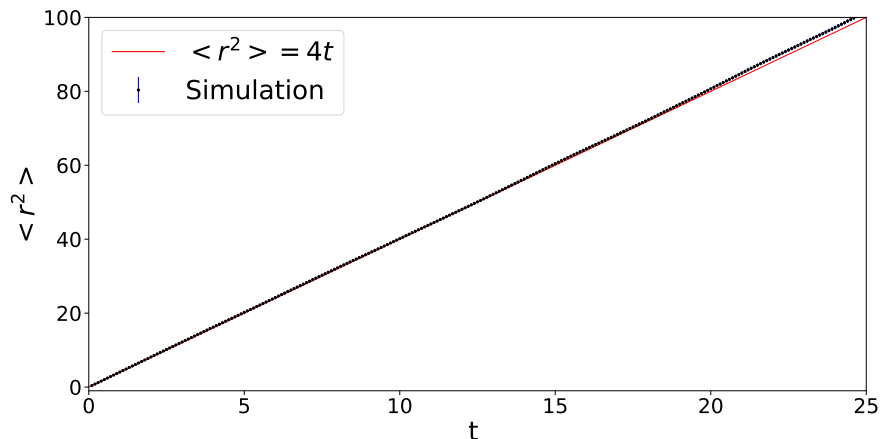


Figure 6: Mean squared displacement in terms of particle diameter as a function of time in terms of diffusion time for active disks. The curves serve as guide to the eye for the data points of expected values and simulated values, as indicated in the legend.

For testing the interaction forces, we added the back interaction forces between particles. It is possible to check if the simulation behaves as expected by comparing the results of the Brownian dynamics simulations with the results from literature and from Monte Carlo simulations. The phase diagram for Hertzian disks is plotted in figure 7. Temperature T in this figure is the same as $k_B T$ used in this thesis and density $\rho = N_{\text{particles}}/A_{\text{box}}$ is the same density as used in our simulations. We look at the configurations at multiple densities. The results for Brownian dynamics are plotted in figure 8. For the set parameters the configurations match with the results found in literature[18]. We also find the same configurations when we perform a Monte Carlo simulation with the same parameters, as can also be seen in figure 8. The Brownian dynamics simulation behaves as expected.

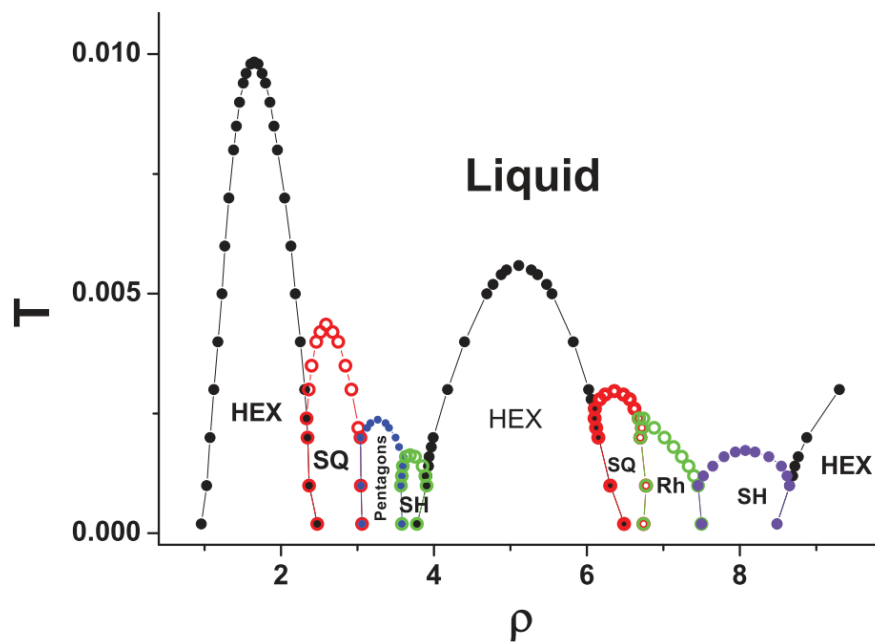


Figure 7: Phase diagram for two-dimensional Hertzian potential particles. Temperature $k_B T$ on y -axis against density ρ in terms of particles per disk diameter squared on x -axis. Figure taken from [18] with permission from Taylor & Francis.

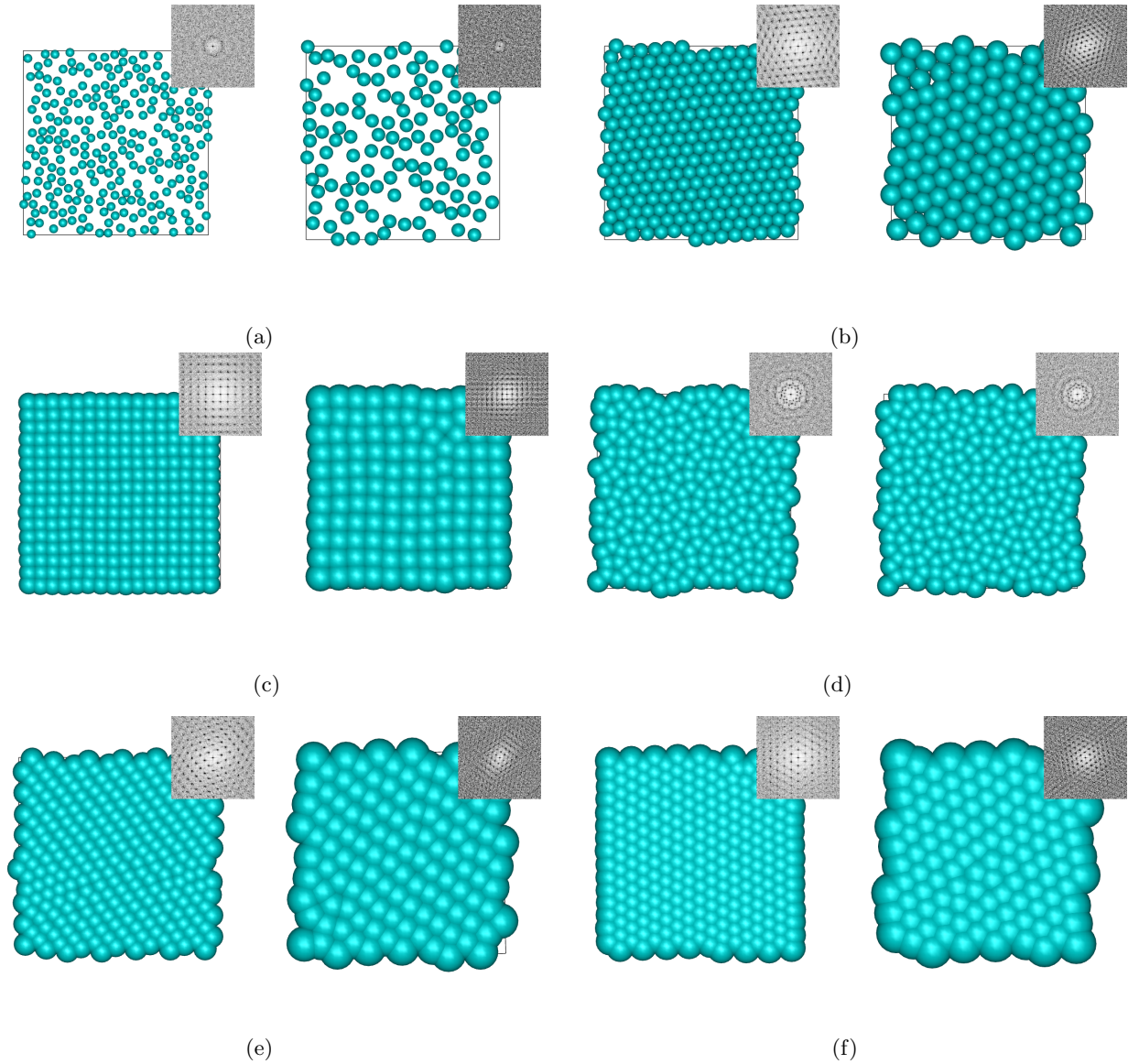


Figure 8: Snapshots of simulations of Hertzian colloids with diffraction patterns at multiple densities. Generated using a Brownian dynamics simulation, figure on the left side, and a Monte-Carlo simulation, figure on the right side. (a) $\rho = 0.6$, fluid phase. (b) $\rho = 1.6$, square crystal phase. (c) $\rho = 2.8$, square crystal phase. (d) $\rho = 3.4$, dodecagonal quasicrystal. (e) $\rho = 3.7$, stretched triangular crystal phase. (f) $\rho = 5.4$, dense triangular phase.

4 Results

In this section we will show the outcomes of the simulations. We will first show the effect of density on the diffusivity of systems of disks and dumbbells. We then study the effect of adding activity to the particles. For a selection of densities we show the result of cell size oscillation and dumbbell length oscillations on the diffusivity of the system. We will inspect if under any of the chosen parameters jamming occurs.

4.1 Passive Particles

Simulations on passive disks produced the MSD's as plotted in figure 9. At a density of $\rho = 1.0$ the MSD increases linearly, which indicates that the system is linearly diffusive. However, at $\rho = 1.8$ the MSD is almost constant for small time steps. After a small increase from $\langle r^2 \rangle = 0$ at $t = 0$ the MSD plateaus. This indicates that the disks are caged and that the system behaves solid-like. This also follows from figure 10 in which the self-intermediate structure factor is plotted for passive particles. At $\rho = 1.4$ and $\rho = 1.8$ F_s starts plateauing starting at $t = 60$. A snapshot of the simulation, figure 11, shows that the polydisperse disks are in a triangular-like lattice. This therefore is not jamming, as the disks are not in a disordered phase.

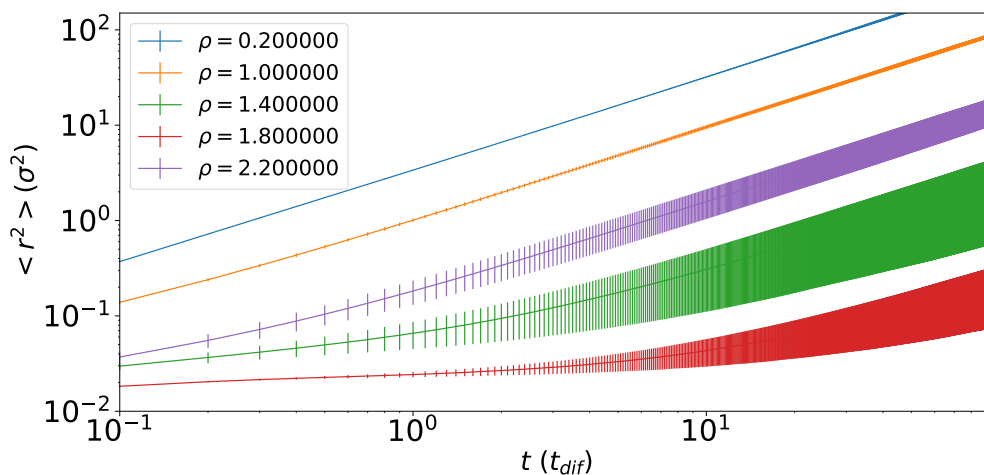


Figure 9: Mean squared displacement in terms of particle diameter as a function of time in terms of diffusion time for passive disks. The curves serve as guides to the eye for data points at different densities as indicated in the legend. The vertical bars indicate standard error.

Simulations of passive dumbbells produced figure 12, in which the MSD's of the simulated systems are plotted. The MSD increases linearly at all densities, which indicates linear diffusion. None of the dumbbell systems are therefore jammed. The linear diffusion is largest at the low density $\rho = 1.0$. The diffusion decreases until the density of $\rho = 1.8$. As density increases further the diffusion increases as well, although it does not reach the levels of diffusivity found at lower densities. The motility of the dumbbell system reaches a low point at a density of around $\rho = 1.8$. The self-intermediate structure factor, as shown in figure 13, also shows that none of the systems are jammed. None of the curves plateau after a quick decay. At every density F_s decreases towards zero, which indicates that all systems are diffusive.

There is however an issue concerning the error bars of the MSD in figure 12. The error is too large for how gradually the MSD increases, especially at a density of $\rho = 1.4$. We encounter the same problem in figure 9. In figure 14 we can see that the large error is caused by large differences in the MSD between individual runs. These large differences are the result of an error made in creating polydispersity in the simulation. Polydispersity was set up separately for every run, which means that the effective density could differ between runs which were meant to be at the same density. In figure 15 the relation between the total area of the particles per run is plotted against the diffusion coefficient at density $\rho = 1.4$. At a larger total area D/D_{average} becomes smaller. The larger error does however not prevent us from being able to analyse

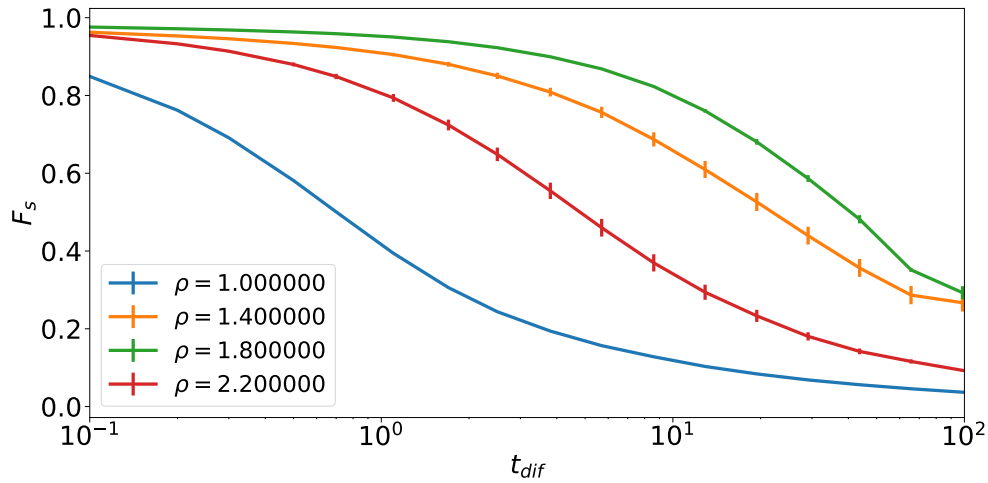


Figure 10: Self-intermediate structure factor as a function of time in terms of diffusion time for passive disks. The curves serve as guides to the eye for data points at different densities as indicated in the legend. The vertical bars indicate standard error.

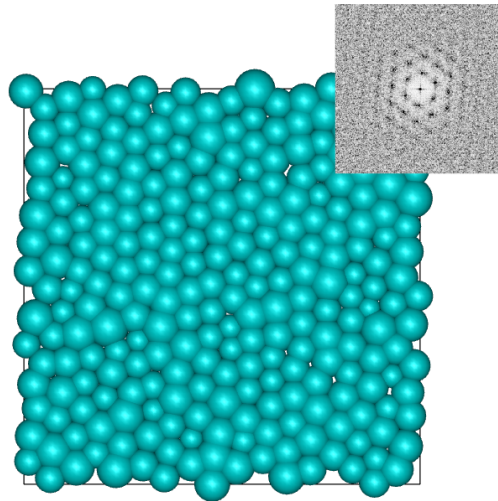


Figure 11: Snapshot of a simulation of passive disks at $\rho = 1.8$. Diffraction pattern of structure is included in top right corner.

the data. The density change caused by this error is not as large as the differences between the densities at which runs have been performed. We can still analyse the differences between systems at different densities. We determined the linear diffusion coefficient of every system. The linear diffusion coefficient for passive dumbbells is plotted in figure 16. The diffusion coefficient decreases as density increases until $\rho = 1.8$. As density increases, a dumbbell interacts more with other dumbbells. This restricts the motion of the dumbbell, which leads to a lower diffusion coefficient. There is a slight increase in the diffusion coefficient however as density increases further. In the diffraction pattern of a system at $\rho = 1.8$, as plotted in figure 17b, a ring like structure is clearly visible. This indicates that the system behaves fluid-like. At $\rho = 3.0$ this structure is not present, which would indicate gas-like behaviour. From figure 17c we can see that at higher densities such as $\rho = 3.0$ overlapping of disks is inevitable. At $\rho = 1.8$ overlapping is rare, but at higher densities

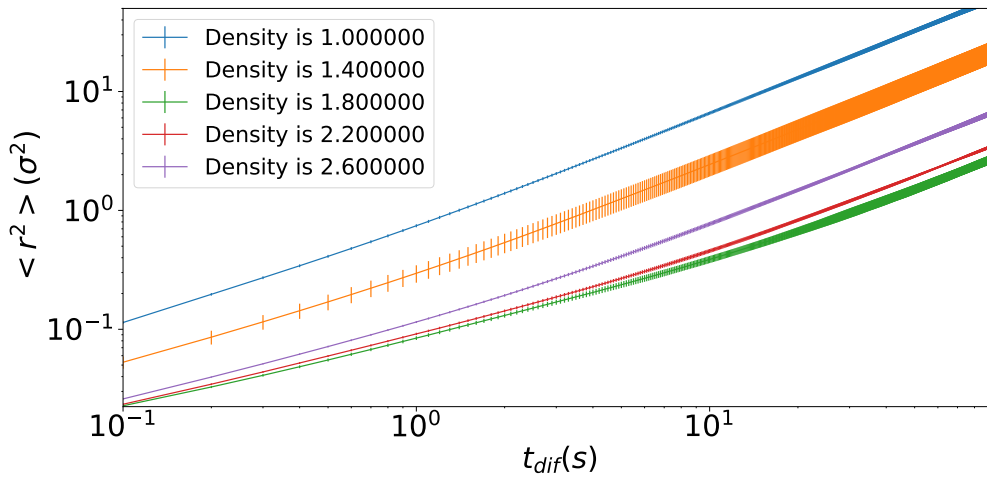


Figure 12: Mean squared displacement in terms of particle diameter as a function of time in terms of diffusion time for passive dumbbells. The curves serve as guides to the eye for data points at different densities as indicated in the legend. The vertical bars indicate standard error.

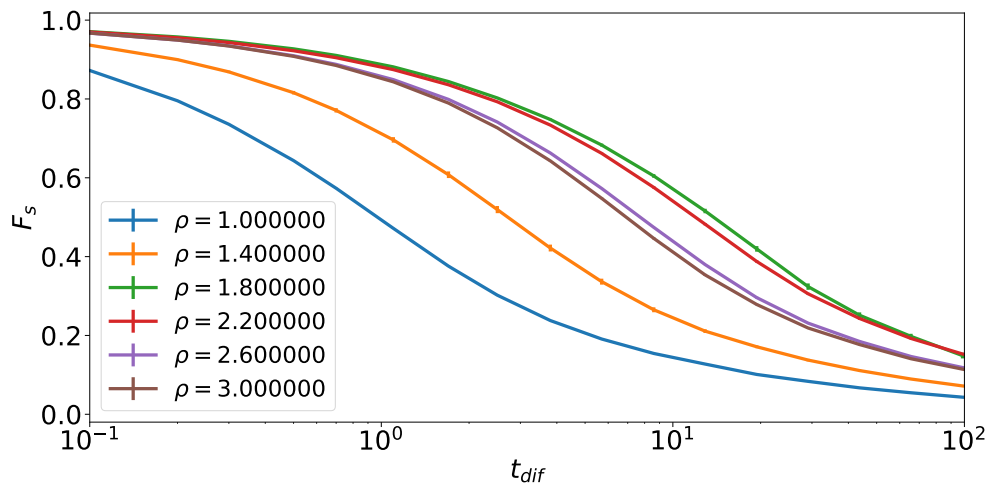


Figure 13: Self-intermediate structure factor as a function of time in terms of diffusion time for passive dumbbells. The curves serve as guides to the eye for data points at different densities as indicated in the legend. The vertical bars indicate standard error.

particles always overlap with neighbouring particles. Hence at high densities particle movement is not caused by single particle collisions, but by the total force exerted on a single dumbbell by all neighbouring particles. It could be a consequence of the soft Hertz potential that at higher densities particles are less restricted in their movement by other particles, compared to slightly lower densities. The Hertz potential is namely not a diverging potential.

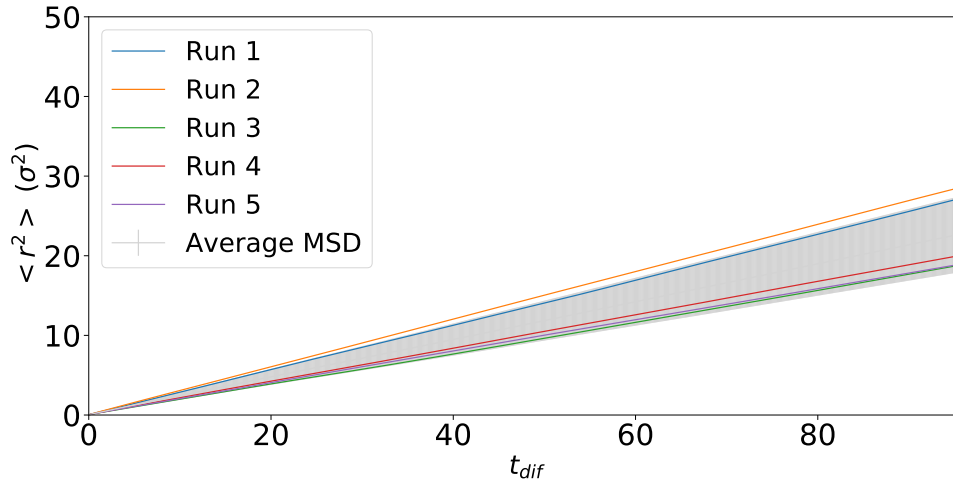


Figure 14: Mean squared displacement in terms of particle diameter as a function of time in terms of diffusion time for passive disks. The coloured curves give the MSD's of individual runs. The grey curve gives the average of these five curves. The area of the grey curve indicates the extent of the standard error of the average MSD.

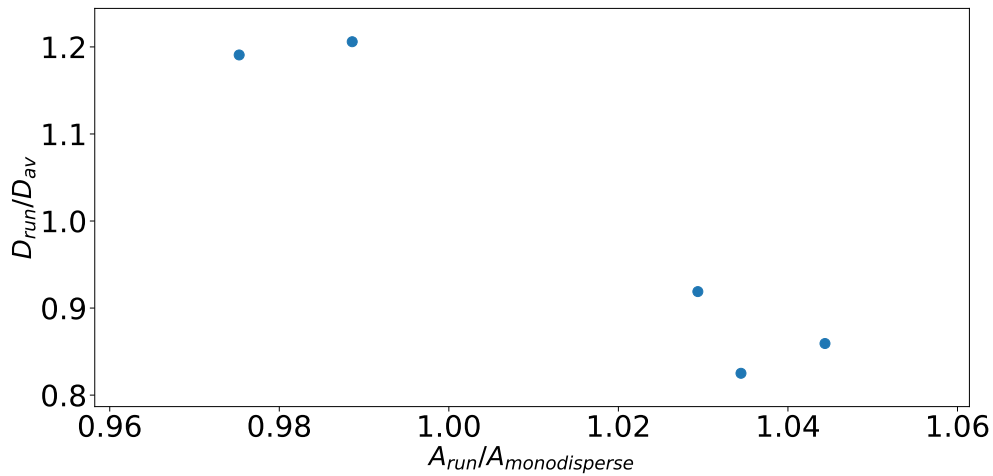


Figure 15: The diffusion coefficient of a run divided by the average diffusion coefficient against the total area of the particles in a run divided by the total area of a run with monodisperse particles. Dots indicate the values of individual runs. All runs were performed at $\rho = 1.4$.

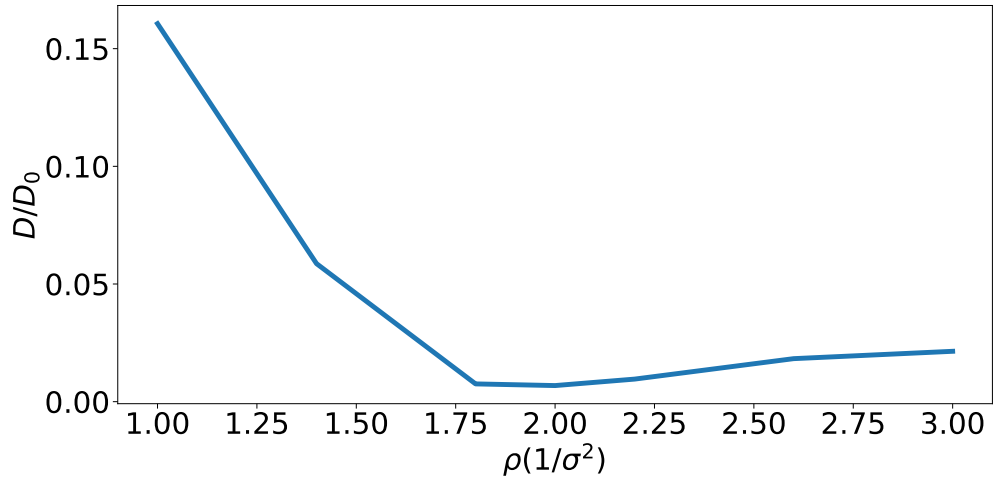


Figure 16: Diffusion coefficient of passive dumbbells divided by diffusion coefficient of interactionless passive disks as a function of density in terms of disks per disk diameter squared.

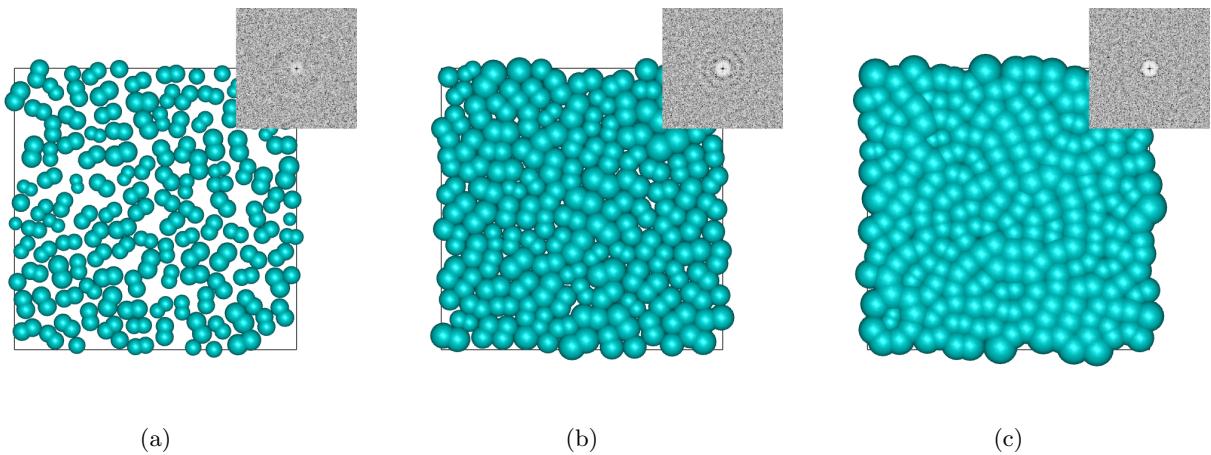


Figure 17: Snapshots of simulations of passive dumbbells with diffraction patterns at different densities. Diffraction pattern of snapshot is included in upper right corner. (a) $\rho = 1.0$. (b) $\rho = 1.8$. (c) $\rho = 3.0$

4.2 Oscillating Particles

We performed simulations on disks with oscillating size. Simulations were done over a range of densities from $\rho = 0.2$ to $\rho = 2.2$ with particles with a diameter oscillation amplitude of $\Delta\sigma = 0.2$. We compared these simulations to the simulations with passive particles. The results of these simulations are plotted in figure 18. The MSD of oscillating disks with amplitude $\Delta\sigma = 0.2$ at $\rho = 1.8$ increases linearly. This system is not jammed, whereas in the system of non-oscillating disks at $\rho = 1.8$ the dynamics had halted, as can be seen in figure 9. The oscillations induce the fluidity of the system. In figure 19 the diffusion coefficient is plotted at multiple densities. Diffusion is increased by adding oscillations to the disks across all densities except very low densities. The jammed system goes from no diffusion to a diffusion coefficient of $D/D_0 = 0.075$.

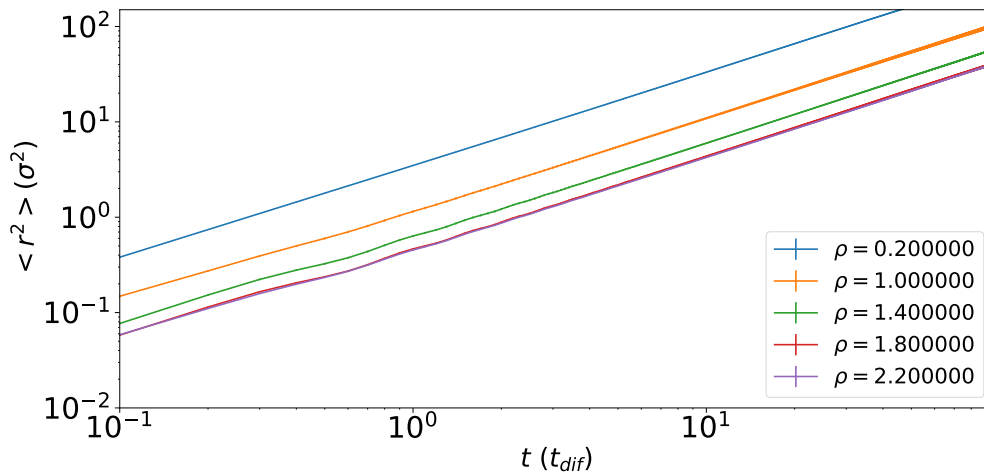


Figure 18: Mean squared displacement in terms of particle diameter as a function of time in terms of diffusion time for active disks. The curves serve as guides to the eye for data points at different densities as indicated in the legend. The vertical bars indicate standard error.

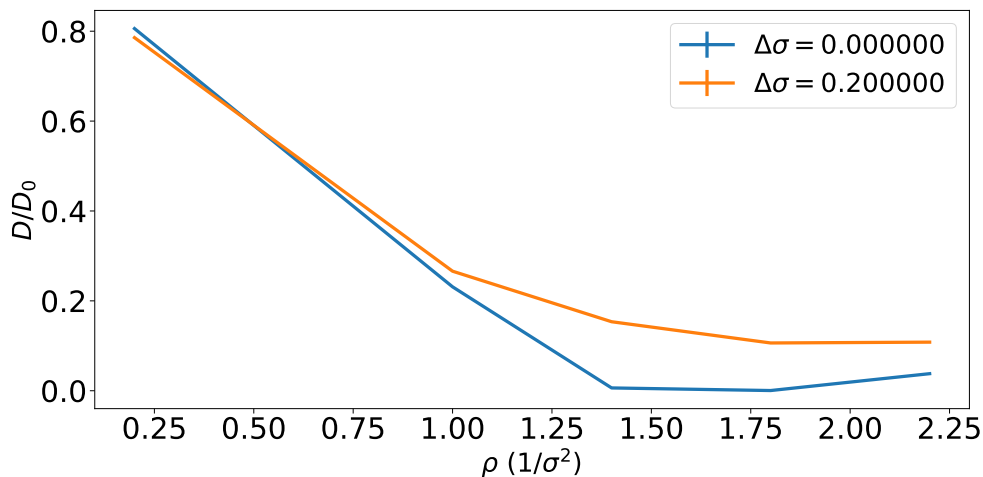


Figure 19: Diffusion coefficient of active disks divided by diffusion coefficient of interactionless passive disks as a function of density in terms of disks per disk diameter squared. The curves serve as guides to the eye for data points for simulations with different amplitudes of diameter oscillation, as indicated in the legend. $\Delta\sigma$ is the amplitude of disk oscillation.

4.2.1 Oscillating Dumbbells

In figure 20 the diffusion coefficient for systems with oscillating dumbbells is plotted. Using this figure we find the effect of the two types of oscillations, length oscillations and disk diameter oscillations. At low densities the effect of oscillations is small. There are namely relatively little particle interactions at these densities. Dumbbell oscillations therefore have little effect on interactions with other particles. The diffusion coefficients of systems with oscillations are comparable to the diffusion coefficients of systems of passive particles. At $\rho = 1.0$ length oscillations increase the diffusion of the system slightly, whereas diameter oscillations decrease the diffusion slightly. The slight diffusion decrease in simulations with diameter oscillations is an effect of the larger effective density caused by these oscillations. For example, two disks with diameter $\sigma = 1.0$ cover a smaller area than one disk with diameter $\sigma = 0.9$ and one with diameter $\sigma = 1.1$. At low densities this larger effective density leads to a small decrease in diffusivity. The diffusivity increase in simulations with length oscillations is caused by the dumbbells extending and pushing away other dumbbells. This process increases the motility of the particles.

At higher densities the effect of oscillations becomes larger. Especially length oscillations have a large effect on the fluidity of a system. At $\rho = 1.8$ the diffusion coefficient D increases sixfold when length oscillations of $\Delta L = 0.2$ are added to the dumbbells. Diameter oscillations have a smaller effect. These only increase the diffusion coefficient by a factor 2.5. Combining the two oscillations leads to a diffusion only slightly larger than the diffusion of a system of dumbbells that only oscillate in length. Length oscillations thus play a larger role in increasing the diffusivity of a system than diameter oscillations. As density increases further the effect of diameter oscillations on diffusivity becomes larger. At high densities the contribution of diameter oscillations to the diffusivity constant approaches the contribution of length oscillations.

At high densities we see that both types of oscillations lead to an increase in diffusivity of the system. The effect of length oscillations stays roughly the same at $\rho > 1.8$. The effect of diameter oscillations however increases as density increases further. As density becomes larger, overlap between disks becomes more prevalent and there are more interactions between particles. Diameter oscillations have a larger effect at higher densities because of the larger number of interactions occurring. In a denser system the force on a particle directed towards a particle of decreasing size is larger, because in all other directions the particle overlaps more with its neighbours. This causes particles to move towards shrinking particles. When there is little to no overlap this process is not as relevant. Diameter oscillations at lower densities mostly increase diffusivity by pushing away other particles while oscillating. This pushing effect is however not as large as

the pushing effect occurring because of length oscillations. This is the case because in our simulation the diameter oscillations are tuned such that the total length of the dumbbell stays constant.

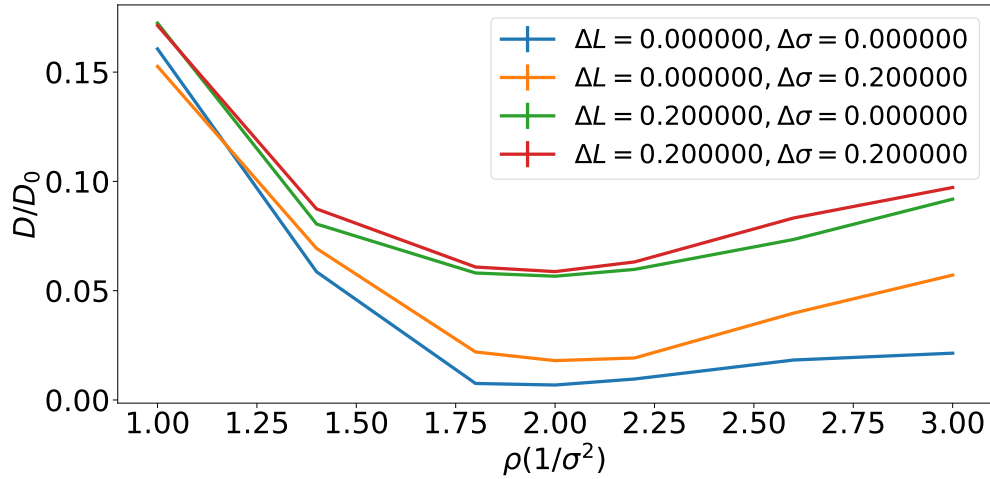


Figure 20: Diffusion coefficient of active dumbbells divided by diffusion coefficient of interactionless passive disks as a function of density in terms of disks per disk diameter squared. The curves serve as guides to the eye for data points for simulations with different types of oscillations and different amplitudes of these oscillation. ΔL is the amplitude of length oscillations, $\Delta\sigma$ is the amplitude of disk diameter oscillations.

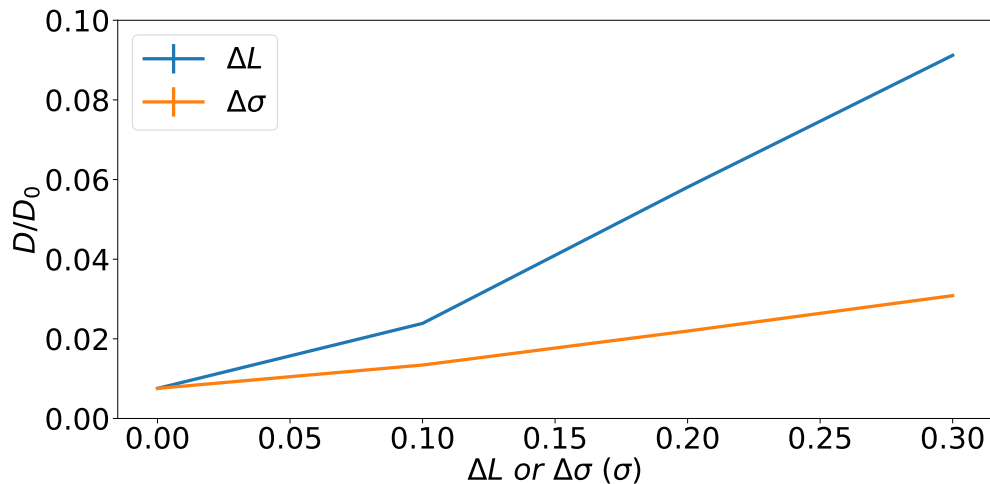


Figure 21: Diffusion coefficient of active disks divided by diffusion coefficient of interactionless passive disks as a function of amplitude of oscillation in terms of disk diameter. The curves serve as guides to the eye for data points for simulations with different types of oscillation as indicated in the legend. ΔL indicates dumbbell length oscillations, $\Delta\sigma$ indicated disk diameter oscillations.

In figure 21 the effect of length oscillations and of diameter oscillations is shown in more detail. An increase in ΔL is associated with an almost linear increase in the diffusion coefficient as well. An increase in $\Delta\sigma$ also increases the diffusivity of the system. However, these diameter oscillations lead to a smaller increase in diffusivity than length oscillations.

5 Discussion

The goal of this thesis was to get more insight into the collective dynamics of epithelial tissue. We modelled deforming cells by building dumbbells out of pairs of soft-potential disks and by tuning the size oscillations of these disks. This model is fairly easy to implement in a simulation. However, even though it is a toy model, it still contains many features of epithelial tissue. The soft repulsive potential used in the simulation allowed for overlapping of particles. In cell tissue the entire tissue area is covered by cells. At sufficiently high densities the particles overlap such that the system resembles an epithelial tissue. Deformations caused by interactions between cells are modelled by interactions and by overlap between particles. The cellular oscillations are modelled in two ways: size oscillations are modelled by dumbbell length oscillations, shape oscillations by disk oscillations. These oscillations in cells are largely autonomous [4], so oscillations of individual dumbbells form a good model.

Using the MSD of the particles in the simulations we determined the diffusion coefficient of the simulated systems. Using the diffusivity coefficient we found the effect of oscillations on the diffusivity of the studied systems. At higher densities, as particles interact more with each other, the diffusivity increased as oscillations were introduced to the particles. Length oscillations and disk oscillations to a lesser degree increased particle motility by pushing away neighbouring particles. This indicates that autonomous cell oscillations increase the diffusivity of fluid-like behaving cell tissue.

We found that for passive and active dumbbell-systems alike the diffusivity was smallest at a density of around $\rho = 1.8$. At higher densities, as overlapping of particles became more prevalent, the diffusivity increased slightly. At this point the system became similar to confluent tissue, as that the area was completely filled with cells. This can only occur in systems of soft particles, because these high densities can only exist because of overlapping. The Hertz potential is a non-diverging potential, so overlap between particles is not as restricted as in systems with hard-potential particles. Dumbbells at higher densities seem to act gas-like instead of fluid-like at these higher densities. Because the dumbbells always overlap with other dumbbells in all directions, an effective pressure acts on the dumbbells. Individual interactions do not have the same influence on the motion of a dumbbell as they have at lower densities. In this gas-like regime the dumbbells are less restricted in their motion. The effective pressure on the particles induces movement if an empty spot is near a particle. This can for instance occur because of disk oscillations in a dumbbell. This explains why the diffusivity increase caused by disk oscillations is larger at higher densities

There were some aspects of the simulation that prevented us from effectively answering the research question. These aspects are outlined below, such that future researchers can benefit from these realizations.

The first issue was a systematic error, which was already discussed in the results section. The effective density in multiple runs of simulations at the same density could differ, because of a mistake in implementing polydispersity. This led to the MSD having a large error. However this did not affect the results in a major way.

In this thesis we were interested in jamming in cell tissue, which had been observed in experiments. It turned out that for simulations with dumbbells we did not observe jamming. We were therefore not able to determine the influence of cell oscillations on jammed systems from simulations. We have the following suggestions for realizing jamming behaviour in future experiments.

The first suggestion is changing the potential of the particles. A possible cause for the absence of jamming lies in the hardness of the potential. Even though jamming has been simulated in systems of Hertzian spheres, overlapping of particles could be a reason for the absence of jamming in our simulations. The cage to which particles are restricted is less clearly defined in systems consisting of soft-potential particles compared to systems of hard potential particles. In a system of disks we did encounter plateauing of the MSD, which indicates that jamming had occurred. This would mean that the softness of the potential cannot be the only reason for the absence of jamming. The disks however were configured to a pseudo-triangular lattice and not to a disordered state.

The second suggestion is to use a different method in constructing dumbbells. The dumbbells are created by connecting two disks with a spring potential. This potential depends on the distance between the two disks. It allows for slight variations in the distance between the disks, even if the equilibrium distance stays constant. Jamming has been simulated in systems with dumbbells with a rigid connection between the two disks[14]. Dumbbells with a rigid connection between the two disks might be a better choice for modelling

cells.

A third suggestion is to perform a non-thermal simulation. We may have overestimated the influence of thermal fluctuations on the motion of cells. We used Brownian dynamics to simulate the motion of the particles, which includes thermal fluctuations. We therefore technically look for glassy behaviour in the studied systems. It could be possible that systems of dumbbells never show glassy behaviour. If we want to achieve a halt of dynamics, it may be necessary to use a purely mechanical simulation without thermal fluctuations in the motion of the particles. This can be done using our current situation by setting temperature to $k_B T = 0$. By implementing this simple change thermal fluctuations in the motion of particles disappear. In this non-thermal model we would actually seek jamming behaviour instead of glassy behaviour. Comparing the results of these two models could give more insight in the behaviour of cell tissue.

Even though we did not observe jamming behaviour, the method used was functional for studying the effect of cell oscillations at different densities. It is possible to study fluid-like tissue using the soft-dumbbell model. We also know that jamming can be simulated in systems of dumbbells if some changes are made to the model. As a toy model a Brownian simulation of dumbbells is very useful. We saw from our simulation results that systems of dumbbells which were similar to confluent tissue, behaved like a fluid. Experiments have shown that epithelial cells behave liquid-like[1]. The results found from our simulations therefore are not in contradiction with experimental results. The current model only did not allow for studying jamming in epithelial tissue.

6 Conclusion

In this thesis a model of soft-potential disks and a model of soft-potential dumbbells were used to study epithelial cells. The effect of oscillations on the collective dynamics of a system of cells was analysed. From our simulation we found that cell oscillations do in general increase the diffusivity of systems of cells

We performed Brownian dynamics simulations with polydisperse soft-potential disks and simulations with polydisperse dumbbells, consisting of two connected soft-potential disks. Diameter oscillations could be added to the simulations performed with disks. In simulations with dumbbells we could add length oscillations to the dumbbells and diameter oscillations to disks that make up the dumbbells.

In simulations with soft-potential disks we observed halting of dynamics at high densities. Systems that were normally jammed however became unjammed when diameter oscillations were added to the disks.

We did however not observe jamming in simulations with passive dumbbell particles. All studied dumbbell systems were linearly diffusive. The diffusivity of the system did change with density. It decreased as density increased until $\rho = 1.8$, but at even higher densities there was a slight increase in diffusivity. This probably was an effect of the large amount of overlapping of particles occurring at higher densities.

When oscillations were added to dumbbell particles the diffusivity increased. At low densities these oscillations had little influence on the dynamics of the system. At densities larger than $\rho = 1.8$ the influence became much larger. Dumbbell length oscillations led to large increases in the fluidity of the system. Disk diameter oscillations also caused increases in diffusivity, but these increases were much lower than the increases caused by length oscillations. At higher densities the contribution of diameter oscillations to the diffusivity of the system became larger and approached the contribution of length oscillations. Diameter oscillations only lead to larger particle motility when particle overlap is more prevalent. For length oscillations to increase diffusivity overlapping of particles is not as important.

For future research it is interesting to investigate why we did not encounter jamming. We can perform simulations with a different type of dumbbell with a stiffer potential. It is also interesting to perform non-thermal simulations and compare the results with the results of this thesis. Once we find under what circumstances simulations with dumbbells jam, we can investigate the influence of cell oscillations on jamming behaviour.

References

- [1] Linda Oswald, Steffen Grosser, David M Smith², and Josef A Käs. “Jamming transitions in cancer”. In: *Journal of Physics D: Applied Physics* 50.48 (2017).
- [2] Thomas E. Angelini, Edouard Hannezo, Xavier Trepant, Manuel Marquez, Jeffrey J. Fredberg, and David A. Weitz. “Glass-like dynamics of collective cell migration”. In: *Proceedings of the National Academy of Sciences of the United States of America* 108.12 (Mar. 2011), pp. 4714–4719.
- [3] Simon Garcia, Edouard Hannezo, Jens Elgeti, Jean-François Joanny, Pascal Silberzan, and Nir S. Gove. “Physics of active jamming during collective cellular motion in a monolayer”. In: *Proceedings of the National Academy of Sciences of the United States of America* 112.50 (Dec. 2015), pp. 15314–15319.
- [4] Nicole Gorfinkiel. “From actomyosin oscillations to tissue-level deformations”. In: *Developmental Dynamics* 25.3 (Oct. 2015), pp. 939–946.
- [5] Guy B. Blanchard, Sughashini Murugesu, Richard J. Adams, Alfonso Martinez-Arias, and Nicole Gorfinkiel. “Cytoskeletal dynamics and supracellular organisation of cell shape fluctuations during dorsal closure”. In: *Development* 137.16 (2010), pp. 2743–2752.
- [6] Yusuke Hara. “Contraction and elongation: Mechanics underlying cell boundary deformations in epithelial tissue”. In: *Development, Growth & Differentiation* 59.5 (July 2015), pp. 340–350.
- [7] James S. Lowe and Peter G. Anderson. *Stevens & Lowe’s Human Histology*. 4th ed. Philadelphia, PA: Elsevier/Mosby, 2015. ISBN: 9780702062933.
- [8] Étienne Fodor, Vishwajeet Mehandia, Jordi Comelles, Raghavan Thiagarajan, Nir S. Gov, Paolo Visco, Frédéric van Wijland, and Daniel Riveline. “Spatial Fluctuations at Vertices of Epithelial Layers: Quantification of Regulation by Rho Pathway”. In: *Biophysical Journal* 114.4 (Feb. 2018), pp. 939–946.
- [9] Andrea J. Liu and Sidney R. Nagel. “The Jamming Transition and the Marginally Jammed Solid”. In: *Annual Review of Condensed Matter Physics* 1 (2010), pp. 347–369.
- [10] V. Trappe, V. Prasad, Luca Cipelletti, P. N. Segre, and D. A. Weitz. “Jamming phase diagram for attractive particles”. In: *Nature* 411 (June 2001), pp. 772–775.
- [11] Andrea J. Liu and Sidney R. Nagel. “Jamming phase diagram for attractive particles”. In: *Nature* 396 (June 1998), pp. 21–22.
- [12] Daniel Bonn, Morton M. Denn, Ludovic Berthier, Thibaut Divoux, and Sébastien Manneville. “Yield stress materials in soft condensed matter”. In: *Reviews of Modern Physics* 89.3 (2017). 035005.
- [13] Martin van Hecke. “Jamming of soft particles: geometry, mechanics, scaling and isostaticity”. In: *Journal of Physics: Condensed Matter* 22.3 (Dec. 2009). 033101.
- [14] Carl F. Schreck, Ning Xu, and Corey S. O’Hern. “A comparison of jamming behavior in systems composed of dimer- and ellipse-shaped particles”. In: *Soft Matter* 6.13 (2010), pp. 2960–2969.
- [15] Chiara Malinverno et al. “Endocytic reawakening of motility in jammed epithelia”. In: *Nature Materials* 16.5 (May 2017), pp. 587–595.
- [16] Josep C. Pàmies, Angelo Cacciuto, and Daan Frenkel. “Phase diagram of Hertzian spheres”. In: *Journal of Chemical Physics* 131.4 (July 2009). 044514.
- [17] Daan Frenkel and Berend Smit. *Understanding Molecular Simulation: From Algorithms to Applications*. 2nd ed. Bodmin, Great Britain: Academic Press, 2002. ISBN: 3257227892.
- [18] Yu D. Fomin, E.A. Gaiduk, E.N. Tsiok, and V.N. Ryzhov. “The phase diagram and melting scenarios of two-dimensional Hertzian spheres”. In: *Molecular Physics* 116.21-22 (2018), pp. 3258–3270.

Acknowledgements

I would like to thank my supervisor Joost de Graaf for giving advice and guiding me through the project. Thank you for your suggestions and help throughout the entire process. I would also like to express my gratitude to my daily supervisor Meike Bos, for putting me back on track so many times during this project. I would also like to thank Clara Abaurrea-Velasco for providing me with the code for determining the self-intermediate scattering function and for giving more insight into analysing systems of colloids. Finally I would like to pay thanks to everybody who gave me the necessary distractions during these last few months. You have kept me sane during this hectic period.